Computational Materials Science 131 (2017) 44–47

Contents lists available at ScienceDirect

Computational Materials Science

journal homepage: www.elsevier.com/locate/commatsci

Formation of stacking fault tetrahedron in single-crystal Cu during nanoindentation investigated by molecular dynamics

Qitao Liu, Lei Deng, Xinyun Wang *, Jianjun Li

State Key Laboratory of Materials Processing and Die & Mould Technology, Huazhong University of Science and Technology, 1037 Luoyu Road, 430074 Wuhan, Hubei, China

ARTICLE INFO

Article history:
Received 20 September 2016
Received in revised form 15 January 2017
Accepted 16 January 2017

Keywords:
Plastic deformation
Stacking fault tetrahedron
Dislocation interaction
Molecular dynamics

ABSTRACT

A novel mechanism without involvement of vacancy or Frank loop is put forward to cast light on the formation of stacking fault tetrahedron (SFT) during plastic deformation of bulk single-crystal Cu with pre-existing parallel coherent twin boundaries (CTBs) via large scale molecular dynamics (MD) simulation. The fresh mechanism is totally different with Silcox-Hirsch mechanism and its sequelae, which supports that to produce an SFT during plastic deformation, formation of Frank loop is not essential in metals with low stacking fault energy (SFE).

1. Introduction

The generation and evolution of defects play a pivotal role in the procedure of plastic deformation in metals and alloys [1]. As a three-dimensional (3D) defect, stacking fault tetrahedron (SFT), enclosed by stacking faults (SFs) on all four {1 1 1} planes and bounded by six stair-rod dislocations [2,3] along its edges, is typical. Although it has been established that quenching, irradiation or plastic deformation [4–12] could introduce SFT, there has been considerable debate on details about mechanisms for the formation of SFT and some researchers are still trying their best to unveil SFT's mystery by high-resolution transmission electron microscopy (HRTEM) [10] and via large-scale molecular dynamics (MD) simulations [13,14,10,11].

To account for the formation of SFTs in samples of quenched gold, Silcox and Hirsch [6] put forward a model, later called Silcox-Hirsch mechanism, as shown in Fig. 1(a). It was concluded that (i) vacancy migration and clustering to produce a Frank loop and (ii) dislocation glide are responsible for the formation of SFT. Though there are still reasonable debates on Silcox and Hirsch's fundamental work [12], Silcox and Hirsch provided a totally considerable mechanism.

Loretto [7,9] proposed a dislocation reaction for the formation of SFT and claimed that vacancies were not involved for tetrahedron formed in deformed metals, which was accepted for many years, see Fig. 1(b). Loretto followed in Silcox and Hirsch's footsteps: formation of Frank loop first occurs, followed by the production of SFT. The difference between the two mechanisms was that how the Frank loop forms. Silcox-Hirsch mechanism was via vacancies clustering, while Loretto's was via a conservative dislocation glide process without diffusion.

Recently, Wang et al. [10] and Li et al. [11] also propounded mechanisms for the formation of perfect SFT in Au and Cu, respectively, which yield low stacking fault energy (SFE) (less than 50 $mJ \cdot m^{-2}$, see Table 1). Wang et al. [10] suggested that three sequential SFs nucleate and interact in pair create an initial open-SFT with only three completed faces and a closed SFT finally forms via the cross-slip of one of the trailing partials into the open (1 1 1) plane, which is critically reviewed and considered flawed [12]. Li et al. [11] reported a dislocation-based mechanism of SFT formation initiated from the semi-coherent interfaces of Cu-Al nanoscale multilayered metals. The recent two mechanisms share a common point that no Frank loop occurs, obviously different with the precursors, however, there still are similarities between the two and Silcox-Hirsch's that three indispensable Shockley partial dislocations bend on the equivalent, inclined {1 1 1} planes, interact in pair. Loretto [7,9] reported that SFTs were observed after deformation at room temperature in the specimens of Ag, Au, Cu et al., which yield low SFE, and no tetrahedra was observed in Al and Ni, which yield high SFE (more than 120 $mJ \cdot m^{-2}$, see Table 1). However, according to Loretto's conjecture, the formation of Frank loop is essential. An obvious gap between Loretto's mechanism [7,9] and Wang's [10] or Li's [11] is left. (Note that it has been reported that under extreme conditions, the formation of

* Corresponding author.
E-mail address: wangxy_hust@163.com (X. Wang).

http://dx.doi.org/10.1016/j.commatsci.2017.01.021
0927-0256/

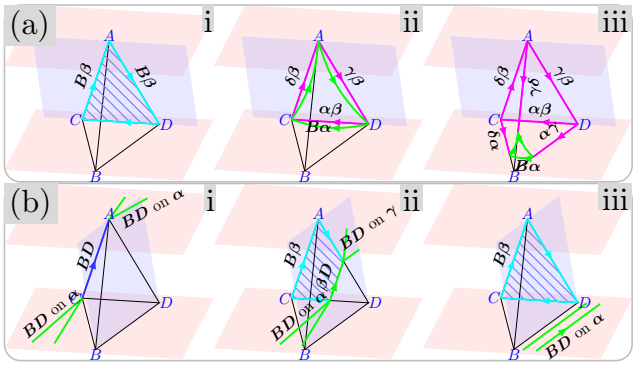

Fig. 1. All the colored lines represent dislocation lines: blue lines stand for perfect dislocations, green for Shockley partial dislocations, magenta for stair-rod locks, cyan for Frank partial dislocations. Arrows are positive directions along dislocation lines. Planes filled with color are shown to clarify geometry: (a) and (b) The planes filled with light red represent α planes, (a) The planes filled with light blue represent β planes, (b) The planes filled with light blue represent γ planes. (a) and (b) The Frank loops are hatched. (a) Dislocation viewpoint of SFT formation, first proposed by Silcox and Hirsch [6]. (b) Mechanism proposed by Loretto [7], depicting the successive steps in the formation of a triangular Frank loop. The jog along *AC*, perpendicular to ***BD***, dissociates to form ***Bβ*** and ***βD***. For much more details, the reader is referred to the text and the original literatures, respectively. For interpretation of color, the reader is referred to the web version of this article. (For interpretation of the references to colour in this figure legend, the reader is referred to the web version of this article.)

Table 1
Summary of SFE of some fcc metals.

	SFE ($mJ \cdot m^{-2}$)
Ag	16.3 [18], 25 [19]
Au	45 [20]
Cu	40 [19], 44.4 [21], 45 [22]
Ni	125 [21,23], 150 [19]
Al	120–144 [24,25], 146 [26], 166 [23]

SFTs in Al [15,16] and Ni [17] was observed. But in the present work, we focus on metals with low SFE.)

2. Computational method

The present work focuses on the nanoindentation of single crystal Cu with ⟨1 1 1⟩ growth orientation and parallel coherent twin boundaries (CTBs). It is straightforward to construct the model for nanotwinned single crystal Cu sample by repeating Σ3 coherent twins in the ⟨1 1 1⟩ axis orientation. The twin boundary spacing was equal to 5.0 nm. The size of the model was $76.6 \times 79.6 \times 40.0\ nm^3$ in the *x*, *y* and *z* directions, made by about 20 million Cu atoms. The indenter was placed above the center of the workpiece with a gap of 3 nm and viewed as a rigid hemispherical diamond shell whose outer radius was 10.0 nm, so the C-C atomic interactions within indenter were ignored. An embedded atom method potential, contributed by Mishin et al. [26], was adopted to model the Cu-Cu atomic interactions. The indentation was modeled using morse potential whose parameters were set as the cohesive energy $D = 0.1$ eV, the elastic modulus $\alpha = 1.7\ Å^{-1}$ and the equilibrium distances $r_0 = 2.2$ Å between atoms *i* and *j* [27]. The cut-off radius of the morse potential was chosen to be 6.5 Å to ensure the computational efficiency.

Three layers of Cu atoms were fixed at the bottom of the workpiece. The above two adjacent layers of thermostat atoms were kept at a constant temperature of 298 K by velocity scaling method for heat dissipation, while the rest atoms were Newtonian atoms. A time step of 1 fs was adopted and lateral periodic boundary conditions were applied in the 3D MD simulation. After initial construction, the model was relaxed using an energy minimization with a conjugate gradient method, and then gradually heated up to the desired temperature 298 K in a step-wise fashion. Indentation was carried out by using LAMMPS at 298 K along the ⟨1 1 1⟩ axis orientation at a rate of $34\ m \cdot s^{-1}$. Dislocation Extract Algorithm [28] was adopted here to analyze the dislocation patterns. All the subsequent discussion utilized Thompston's notation [29] for the Burgers vectors. For more details of the modeling method refer to our published work [30].

3. Results

Supplementary movie shows the formation of an SFT above the CTB, and the last frame of Supplementary movie is as depicted in Fig. 2. When the indentation depth reaches 12.7 Å, a perfect SFT forms. It could be concluded that no vacancy or Frank loop is involved.

The corresponding dislocation mechanism is schematically shown in Fig. 3. Twin boundaries can act as dislocation barriers during plastic deformation [31], which causes the nucleus (i.e. a special dislocation configuration above the CTB) to form a SFT: The dissociation of perfect dislocation ***AC*** into Shockley partial dislocations ***βC*** and ***Aβ*** on plane β and the dissociation into ***δC*** and ***Aδ*** on plane δ are connected by a perfect dislocation ***AC*** which is constricted by stress along *BD* as shown in Fig. 3(a). With the increasement of stress, the partials ***βC*** and ***Aβ*** dissociate on planes α and γ, respectively. The two reactions could be summarized, respectively, as

$$\boldsymbol{\beta C} \rightarrow \boldsymbol{\beta\alpha} + \boldsymbol{\alpha C} \tag{1}$$

and

$$\boldsymbol{A\beta} \rightarrow \boldsymbol{A\gamma} + \boldsymbol{\gamma\beta}. \tag{2}$$

At the same time, another reaction [3] should be presented here, i.e.

$$\boldsymbol{AC} \rightarrow \boldsymbol{A\gamma} + \boldsymbol{\gamma\alpha} + \boldsymbol{\alpha C}. \tag{3}$$

The three reactions are shown in Fig. 3(b), resulting in the formation of an open-ended SFT. Then ***αC*** would glide on the α plane till it reaches the line *BC*. ***AC*** dissociates into Frank partial ***Aα*** along *BD* while stair-rod dislocation ***βα*** elongates, see Fig. 3(c), which could be written as $\boldsymbol{AC} \rightarrow \boldsymbol{A\alpha} + \boldsymbol{\alpha C}$. The succedent action is that ***Aγ*** glides to achieve the line *AB*. Another dislocation dissociation, i.e.

$$\boldsymbol{A\alpha} \rightarrow \boldsymbol{A\gamma} + \boldsymbol{\gamma\alpha} \tag{4}$$

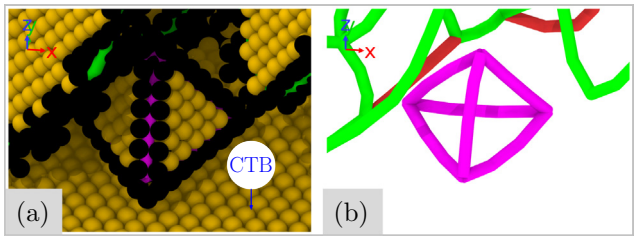

Fig. 2. When the indentation depth reaches 12.7 Å, a perfect SFT forms. Bold colored lines represent dislocation lines: green lines stand for Shockley partial dislocations, magenta for stair-rod locks, red for other dislocations. (a) Atoms in perfect face-centered cubic (fcc) configuration are removed and atoms are colored based on the following scheme: yellow for hexagonal close packing (hcp) atoms, black for other atoms including surface atoms and dislocation cores. CTB is marked. (b) SFT made up by six stair-rod partial dislocations. For interpretation of color, the reader is referred to the web version of this article. (For interpretation of the references to colour in this figure legend, the reader is referred to the web version of this article.)